Tribol Lett (2016) 64:2
DOI 10.1007/s11249-016-0726-3

ORIGINAL PAPER

Observation and Analysis of Micro-Behavior Characteristics and Element Contents during Boundary Layer Evolution under Powder Particulate Lubrication

Bin Yang[1] · Wei Wang[1] · Kun Liu[1] · Yong Liu[1]

Received: 14 October 2015 / Accepted: 22 July 2016 / Published online: 23 August 2016

Abstract Typical characteristics of the boundary layer under powder lubrication are microscopic reflections of lubrication states and closely related to lubrication properties. Therefore, the current investigation is focused on the changes in typical features of boundary layer with an annular contact, flat-on-flat sliding. A 3D laser profile gauge, scanning electron microscopy, X-ray energy-dispersive spectrometer, and Raman laser confocal spectrometer are utilized to microscopically observe and analyze the boundary layers formed on the brass specimens during the process of graphite-lubricated 0.45 C steel (HRC56) sliding upon brass alloy (H62). The evolution of mixed powder lubrication can be divided into four typical stages: (A) running-in, (B) stable, (C) deterioration, and (D) damage. Accompanied by better lubrication performance, the boundary layers are flat and the surfaces are smooth at early stages. Meanwhile, the surface roughness keeps low level, and the carbon content is consistent. Then, the surface flatness worsens gradually and the surface roughness containing boundary layer increases. Simultaneously, the carbon content on the surface decreases, and the copper content becomes even more. Along with the deterioration of the lubrication, iron is observed on the lower brass specimen, indicating a significantly direct contact between the upper and lower specimens. Moreover, the graphite powder, which used to be an excellent solid lubrication material, transforms to the disordered state in the test. From the Raman spectrometer analysis, the stable phase is the most feasible graphitization stage coupled with optimal lubricity. Friction characteristics are closely associated with the boundary layer states in powder lubrication, and improving the corresponding conditions can delay the damage processes.

Keywords Friction · Powder lubrication · Boundary layer · Element contents · Carbon structure

1 Introduction

Some solid particles in dry friction are generally distributed between two relative moving surfaces (i.e., coming from surface peeling or external invasion), which are involved in the relative motion of tribopairs and can affect their entire friction characteristics [1–4]. In 1984, Godet [5] proposed the third body to describe these solid particles, and the two corresponding surfaces of tribopairs were called as the first body. Iordanoff et al. [6] noted that the third body could form as a result of the surface peeling or the addition of external lubricants; the third body formed internal particle streams which circulate around the contact area and occasionally produce wear particles.

Further research has shown that dry powder or other types of solid particle lubricants can be added to the clearance of tribopairs. The use of friction, deformation, collision, extrusion, slip rolling, and other microscopic motions of these tiny particles can decrease the direct contact of the asperities on the relatively moving surfaces to reduce friction and wear, as well as protect the surface [7–10]. A new lubrication method has been developed and known as powder lubrication. Scholars have comprehensively studied the friction and wear characteristics in powder lubrication. Many parameters, such as material, surface condition, load, speed, temperature, environment,

✉ Wei Wang
weiwang@hfut.edu.cn

[1] Institute of Tribology, Hefei University of Technology, Tunxi Road 193, Hefei 230009, Anhui, China

contact area, and particle size, have been focused in various studies [11–14].

At first, Heshmat [15] studied the powder film in the lubrication processes by establishing a test rig and determined that a powder film was formed in a narrow tribopair, which showed the similar characteristics as the fluid lubricant. This feature is known as "quasi-fluid" of powder lubrication. Heshmat and Brewe [16, 17] also used MoS_2 and WS_2 powder to conduct a dusting lubrication experiment on a three-pad radial bearing; their results showed that the friction coefficient and friction torque remained stable with the increasing load and speed.

Powder lubricants are also applied to wide areas [18–23]. Descartes et al. [24, 25] used the $MoS_{1.6}$-coating spread on the substrate surface to study the third-body dynamic (i.e., liquidity and rheological properties). One of the first bodies was made up of transparent materials, and the changes in the contact surface were observed directly by an imaging device, particularly the third-body movement. Higgs and Heshmat [26] used the pressed MoS_2 powder bar to test and observe the separation of powder particles; the results showed that the MoS_2 particles can form a film with friction characteristics and fluid properties. Patrick et al. [27] analyzed the sample surface carefully after the test by a 2D or 3D surface topography analyzer and scanning electron microscopy (SEM); their results showed that the main reason for the powder separation was the abrasive wear and friction between the substrate covered with the boundary layer and slider accompanied by the extrusion, deformation, and compaction of powder. Pudjoprawoto et al. [28] established a 3D volume fraction cover model based on the above experiments to predict the friction behavior of the self-lubricating transfer film. The goal is to increase the fidelity in predicting the friction coefficients at the pellet/disk and slider/disk interfaces as functions of the fraction of lubricant covering the disk asperities. Wang et al. [29] used a friction and wear testing machine to study the powder lubrication characteristics of an annular contact; their results showed that powder intervention was affected by the powder types, tribopair structures, and working conditions.

Powder lubrication is gradually applied in the actual project to solve some lubrication problems under extreme conditions which is insurmountable via traditional lubrication. Reddy and Rao [30] and Gopal and Rao [31] continued to import graphite particles with sizes of 2 and 1 μm into the grinding surface, respectively, to solve the pollution problem caused by traditional cutting fluids. Powder lubrication showed enhanced process ability in grinding AISI1045 steel and SiC ceramics and evidently reduced the friction and pollution. Kimura et al. [32] developed a closed cavity die-casting system by using powder lubrication instead of water-based and oil-based lubrication; its practical application showed that the powder material demonstrated suitable lubricity, and the non-volatile and heat insulation of solid powder improved the working environment and decreased the local solidification in the casting. Pinheiro et al. [33] also studied the influence of powder lubrication on the thermal effects and surface quality of minted billets and determined that powder lubrication decreased the thermal conductivity of mold by 50 % compared with oil lubrication.

Particulate lubrication has elicited attention from many scholars. Recent experiments have further studied the macroscopic features while the behavior of particles in microscale is relatively lacking. While many small and confined particles are existed in the lubrication interface, the reunion, shear, bearing, and migration behavior of these particles, as well as the coupling effect of asperities and particles, influence the velocity accommodation mechanism and contact mechanics, which inevitably affected tribological behavior and boundary layer behaviors. Typical micro-characteristics of the boundary layer evolution in mixed powder lubrication are closely related to lubrication properties and microscopic reflections of lubrication conditions. So the current study is focused on the changes in typical features of the boundary layer formed on the brass specimens under powder particle lubrication from the aspect of lubrication interface evolution and keenly analyzes the changes of the roughness, element content, and carbon structure of the boundary layer. This study also reveals the boundary layer evolution, which provides a basis for applications of powder lubrication.

2 Test Conditions

This experiment uses a plane contact tribotester (HDM-20) developed by the Institute of Tribology of Hefei University of Technology (Fig. 1). The right part of Fig. 1 shows a physical photo of the tester; the middle part is a schematic of the clamped specimen, and the left part is a physical photo of the upper and lower specimens. During the experiments, the upper sample keeps rotated, whereas the lower sample is fixed in the fixture. The fixture of the lower specimen is placed on the joint bearings, which plays a role in adjustment to ensure the plane contact. To maintain the same surface roughness, the upper specimen is polished by the same sandpaper before each test, and the upper and lower specimens are washed with acetone. The normal load is applied along the vertical axis of the upper sample. The parameters, such as friction torque (0–10 N m), load (0–20,000 N), and temperature (−30 to 250 °C), could be measured in this test rig. The friction torque and normal load are obtained using two force sensors, and the friction

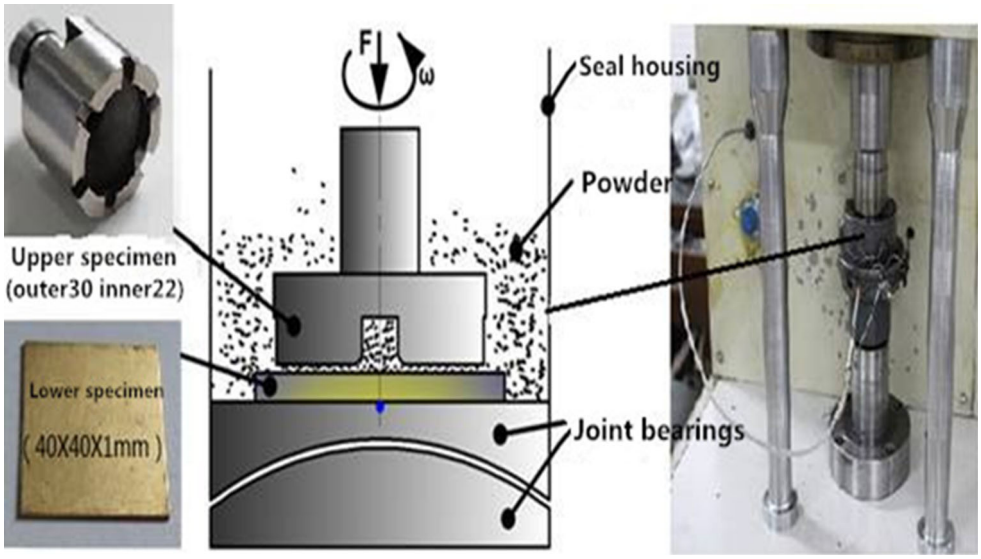

Fig. 1 Schematic of the tester

coefficient is calculated via conversion based on the structural relationship. The temperature could be measured in real time by a thermocouple which is placed at the center of the lower sample. The precision of the friction torque, load, and temperature is ± 0.5 % F.S, ± 1.0 % F.S and ± 0.5 % F.S, respectively. The digital camera, 3D laser profile gauge, SEM, EDS, and Raman laser confocal spectrometer are used to observe and analyze the boundary layers formed on the lower (brass) specimens at different stages.

The outer diameter of the upper specimen is 30 mm, and the inner diameter is 22 mm. The end face is annular with six notches arranged circumferentially, whose width is 4 mm and depth is 3 mm. The structure design reduces the line speed difference on the surface and improves experimental consistency. Besides, the notch structure facilitates the continuous introduction of powder into the lubrication interface. The material is 0.45 C steel with HRC56 hardness after the quenching process. The 3D topography and parameters of the upper specimen surface are presented in Fig. 2a and Table 1. The lower specimen is made of brass alloy (H62) with a size of 40 mm × 40 mm × 1 mm. The 3D topography and parameters of the lower specimen surface are compared in Fig. 2b and Table 1. This experiment uses graphite powder as the lubricant and its lamellar structure to obtain excellent anti-friction and wear resistance. The average size of graphite powder used in the experiments is about 29.17 μm. The experimental conditions are described as follows: The load is 4 MPa; the temperature is 25 °C; the velocity is 0.4 m/s; the amount of graphite powder is 0.8 g; and the relative humidity is about 75 %. Generally, the effects of experimental conditions on the lubrication characteristics and powder layer formation are complicated. The selection of above parameters is based on fore studies [8, 29]. The number of tests repeated is about six to ensure this experiment reliable. All results presented in paper are typical or averaged data from repeated experiments. The amount of graphite powder needed is spread on the lower specimen before every test. Then, the powder could dynamically enter the frictional clearance without any special treatments during the tests.

3 Results and Discussion

3.1 Partition to Lubrication Interface Evolution

After a series of experiments under the same conditions, wear track of the lower specimens after test are observed, analyzed and summarized in detail. Figure 3 shows the curve of friction coefficient changing with time and surface states at a typical moment in the entire test. This figure shows that the friction coefficient initially increases and then decreases to a certain stable value, which is maintained for a long time. And finally, the friction coefficient increases rapidly while damage occurred. According to the repeated tendency of friction coefficient, the entire process can be divided into four typical stages: running-in (A), stable (B), deterioration (C), and damage (D).

Four photos of the surface features at the typical moments acquired are shown in Fig. 3. The friction coefficient at the initial stage, which is the adaptation stage for tribopairs and powder, changes dramatically (from 0 to 0.25). From the surface state of the lower specimen observed at 120 s, there is no complete boundary layer formed on the surface at this stage. While the friction interface and powder lubricant adapt to each other, the frictional interface reaches a steady state, and the friction

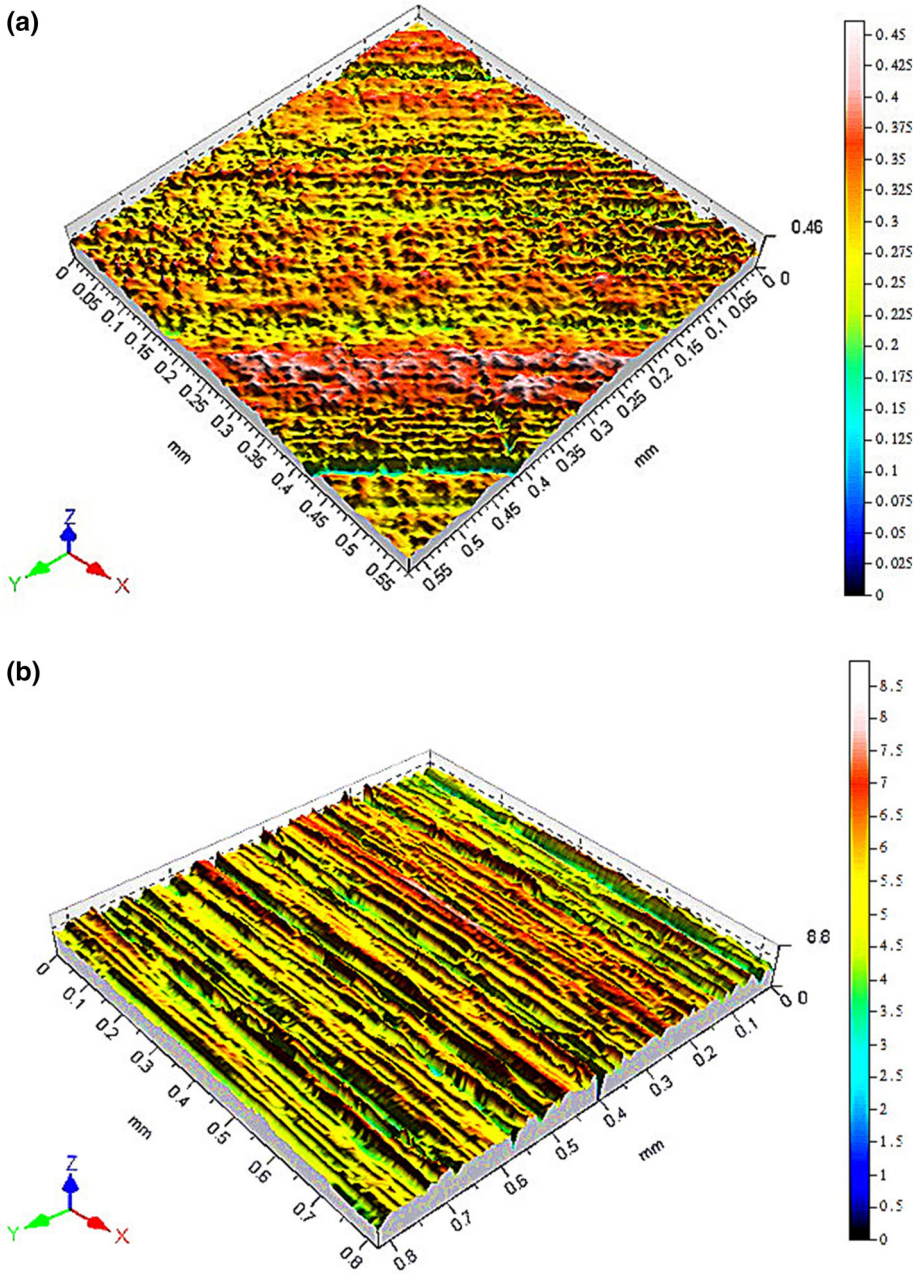

Fig. 2 Surface 3D topography of the upper and lower specimens. **a** Surface 3D topography of upper specimen, **b** Surface 3D topography of lower specimen

Table 1 Original surface topography parameters of the upper and lower specimens

Original surface of specimen	*Sa* (μm)	*Sq* (μm)	*Sz* (μm)	Length (*X*) (mm)	Length (*Y*) (mm)
Upper	0.032	0.042	0.460	0.55	0.55
Lower	0.723	0.931	8.872	0.80	0.80

coefficient changes slightly (between 0.15 and 0.2). Its running time is more than 70 % of the entire time. From the state photo taken at 600 s, a complete boundary layer has formed on the surface at this stage. Due to the deterioration of working conditions, the friction coefficient at the next stage, which is approximately 10 % of the entire time, increases sharply after 1400 s. The state photo of tribopairs is selected at 1620 s when the boundary layer becomes thin and exhibits local loss. The substrate surface comes into contact directly at the final stage, which also aggravates the boundary layer damage till the fully destruction as shown in the state photo at 1722 s. The deterioration of operating

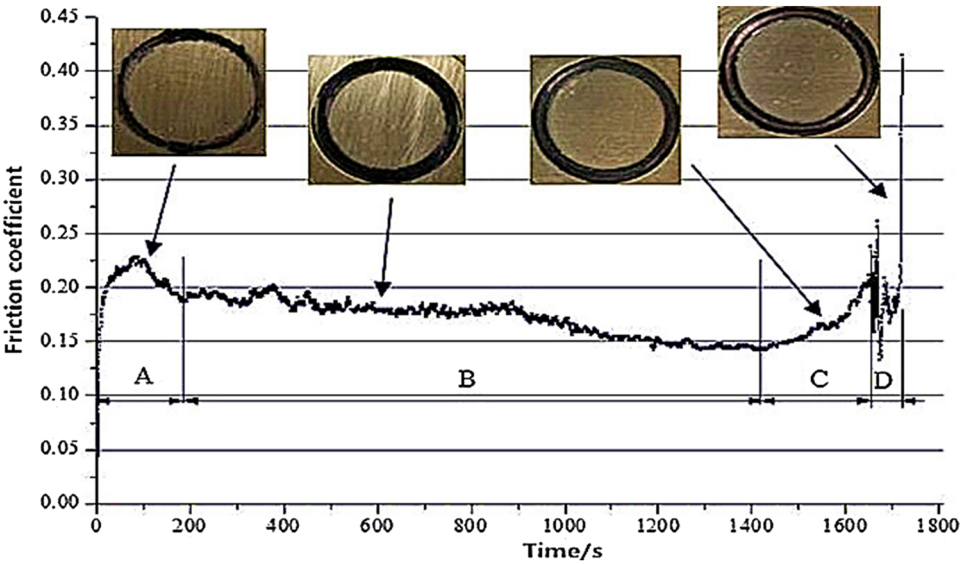

Fig. 3 Curve of the friction coefficient changing with time and surface state under a typical moment

conditions is primarily manifested in particle aggregation and producing an unbalanced friction force.

3.2 Analysis of 3D Surface Topography of Boundary Layer

Surface topography analysis is an important means for the friction and wear test, especially when applied to analyze the boundary layer of the powder lubrication interface. This method plays an important role in the qualitative and quantitative description of the powder state on the surface and can reflect results caused by the movement of particles between the tribopairs, such as extrusion, agglomeration, and dissipation. The relationship between the powder and tribopairs represents the three-body interaction. The boundary layer composed of graphite is relatively soft. Thus, the flatness of the boundary layer can show states of the friction interface and provide more information regarding the powder spreadability and effects of the scratch and plow of asperities.

The 3D laser profile gauge is used to analyze the 3D surface topography of the boundary layer of lower specimen surfaces shown in Fig. 3. The results obtained from four typical stages are shown in Fig. 4 and Table 2. Figure 4a shows the 3D surface topography of the running-in stage. The entire surface is smooth because the powder begins to fill the valley between asperities on the surface. However, some asperities covered by the compacted powder are observed at this stage, which are prominent and higher compared to the flat areas around. Figure 4b–d shows the 3D surface topography of the stable, deterioration, and damage stages, respectively. The surface flatness worsens as operating time increases and finally forms many deep ravines. Some 3D surface parameters of the above stages and original surface are listed in Table 2, showing that the *Sa* of the original surface is 0.723 μm (which is larger than the *Sa* of the running-in, stability, and deterioration stages), and the original *Sz* is 8.872 μm. When the tribopairs run to the damage stage, the *Sa* and *Sz* increase to 2.453 and 21.455 μm, respectively. The boundary layer on surface has become markedly uneven. These results reveal that the surface topography evolution of the boundary layer occurs over time. The lubrication performance is better, when the surface is relatively smoother, namely both the surface roughness and the height difference between the peak and valley of the boundary layer are smaller.

3.3 Analysis of Element Composition of Boundary Layer Surface

Figure 5 presents the SEM microscopic observation results of the same boundary layer surfaces shown in Fig. 3. As shown in Fig. 5a, the carbon layer on the lower surface exhibits an uneven cover, accompanied the phenomenon of graphite agglomeration. The dark area contains more graphite, whereas the gray area has less. As presented in Fig. 5b, c, the surface becomes smoother, and the carbon content is almost consistent. Figure 5d shows the SEM image of the damage stage, whose middle part is the gully region. However, the two sides are planarized regions because of the micro-plastic deformation.

Simultaneously, EDS is used to analyze the element content of the corresponding surfaces in Fig. 5. Table 3 lists the atomic content and mass fractions of five elements (C, O, Cu, Zn, and Fe) in these areas. Figure 5a shows that graphite powder begins to enter the clearance of asperities on the lower specimen surface at the running-in stage, and the powder significantly aggregates. The mass fraction of

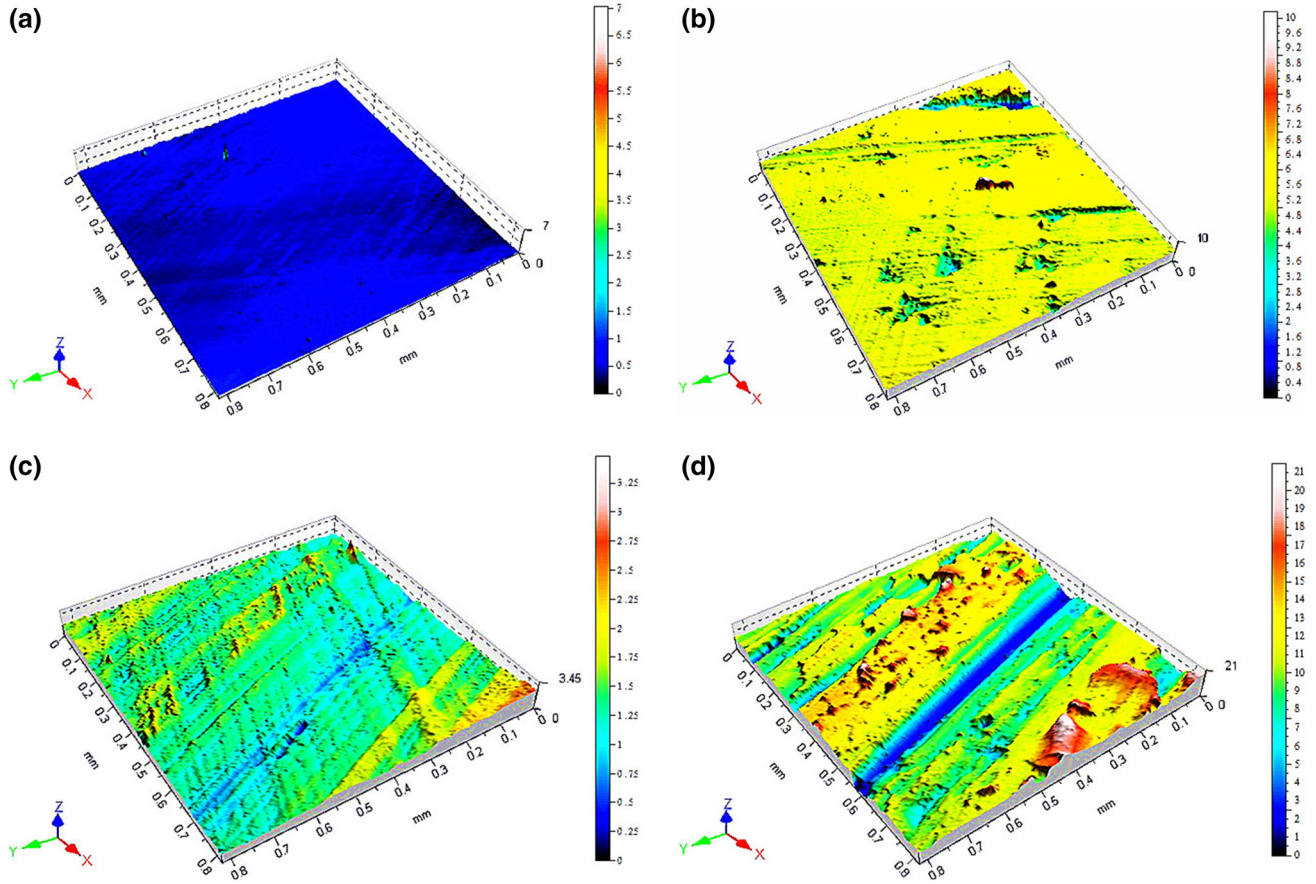

Fig. 4 Surface 3D topography of the boundary layer under a typical moment. **a** 120 s, **b** 600 s, **c** 1620 s, **d** 1722 s

Table 2 Height parameters of the boundary layer surface before and after the test

Surface	*Sa* (μm)	*Sq* (μm)	*Sz* (μm)
Pre-test	0.723	0.931	8.872
120 s	0.106	0.141	7.034
600 s	0.319	0.588	10.176
1620 s	0.601	1.023	14.564
1722 s	2.453	3.214	21.455

carbon is 26.85 %, whereas that of copper is 44.28 %. The entire process enters the stable stage when the boundary layer forms on the lower specimen, as shown in Fig. 5b. The coverage area of the boundary layer increases but becomes thin, whereas that of the copper substrate decreases. Alternatively, the carbon mass fraction decreases to 12.25 %, but the copper mass fraction increases to 48.71 %. When it enters the deteriorating stage as shown in Fig. 5c, the boundary layer becomes thinner and worse because of dissipation. The mass fraction of carbon is 13.37 %, whereas that of copper decreases to 46.49 %. The increasing amount of carbon is attributed to the special structure of the upper specimen, making the graphite powder supplemented. When it enters the damage stage as shown in Fig. 5d, the exposed copper substrate formed by wear and tear covers the whole lower friction surface. The mass fraction of carbon decreases to 1.04 %, whereas that of copper increases to 59.67 %. At this point, iron is detected on the lower brass specimen, and the mass fraction is 0.53 %, showing a significant direct contact between the upper and lower specimens. Thus, the above analysis illustrates that the carbon mass fraction on the lower specimen surface is approximately 12.70 % in normal operation. The friction characteristic is closely associated with the states of the boundary layer in powder lubrication, and the lubrication deterioration and increasing of the wear are closely related to the lack of powder in boundary layers formed in the tribopairs.

3.4 Raman Spectral Analysis of Boundary Layer

Laser Raman spectroscopy, one of the characterization methods to show the change of the carbon material structure, is an important approach to reveal the lubrication properties of graphite lubricant in the evolution process.

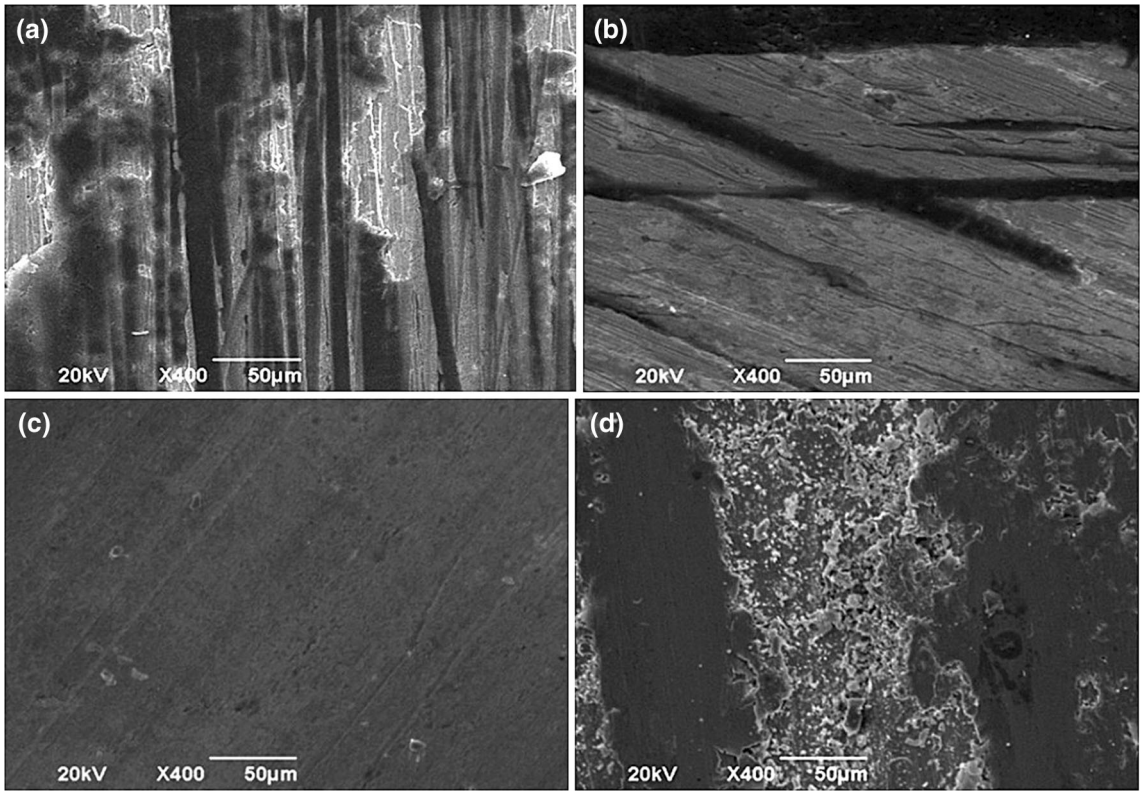

Fig. 5 SEM of the boundary layer surface at a typical moment. **a** 120 s, **b** 600 s, **c** 1620 s, **d** 1722 s

Table 3 Main element content of the boundary layer surface at different stages

Element	Running-in stage		Steady stage		Aggravation stage		Failure stage	
	wt%	at.%	wt%	at.%	wt%	at.%	wt%	at.%
C	26.85	63.37	12.25	37.19	13.37	37.38	1.04	4.37
Cu	44.28	19.75	48.71	27.96	46.49	22.98	59.67	47.45
O	3.26	5.78	7.29	16.62	10.62	22.30	7.44	23.49
Zn	25.61	11.10	31.09	17.34	28.64	16.25	31.32	24.21
Fe	0	0	0	0	0	0	0.53	0.48

This section analyzes the Raman spectra of graphite powder in the four phases showed in Fig. 3, and compared with the original Raman spectra of graphite powder before the test. Then, the effect of the carbon structure on the lubrication properties is studied.

Table 4 lists the Raman analysis results of the corresponding structure parameters of the graphite carbon. Figure 6 shows two peaks (D and G) in the Raman spectra located at approximately 1360 and 1580 cm^{-1}, respectively. Peak D located at 1360 cm^{-1} corresponds to the disordered graphite structure, whereas peak G located at 1580 cm^{-1} corresponds to the ordered graphite structure. The ratio of the two peak intensities (I_D/I_G) can reflect the ordering degree of the carbon material. A smaller ratio indicates a smaller size of the microcrystals, and the crystals are more complete. This condition means that the graphitization degree of the carbon material is higher and the lubrication performance is better. As summarized in Table 4, the original ordering degree of the graphite powder ($I_D/I_G = 0.101$) is smaller than those of phase A ($I_D/I_G = 1.699$), phase B ($I_D/I_G = 1.019$), phase C ($I_D/I_G = 1.878$), and phase D ($I_D/I_G = 1.776$). This finding illustrates that the graphitization degree of the graphite powder worsens after the test. The reason for this is that its complete lamellar structure and microcrystal structure are destroyed during the experiment by the motions, such as the extrusion, inner shearing, grinding and collision et al. Therefore, the graphite powder with significant lubrication performances transforms to the disordered state in the test. Simultaneously, the ordering degree of phase B ($I_D/$

Table 4 Structural parameters of the Raman spectra of graphite particles

Sample	Raman shift		FWHM/D (cm^{-1})	FWHM/G (cm^{-1})	I_D/I_G
	D band (cm^{-1})	G band (cm^{-1})			
Original graphite	1355	1584	36	19	0.101
A	1347	1578	93	77	1.699
B	1349	1581	191	55	1.019
C	1344	1587	106	87	1.878
D	1345	1586	120	85	1.776

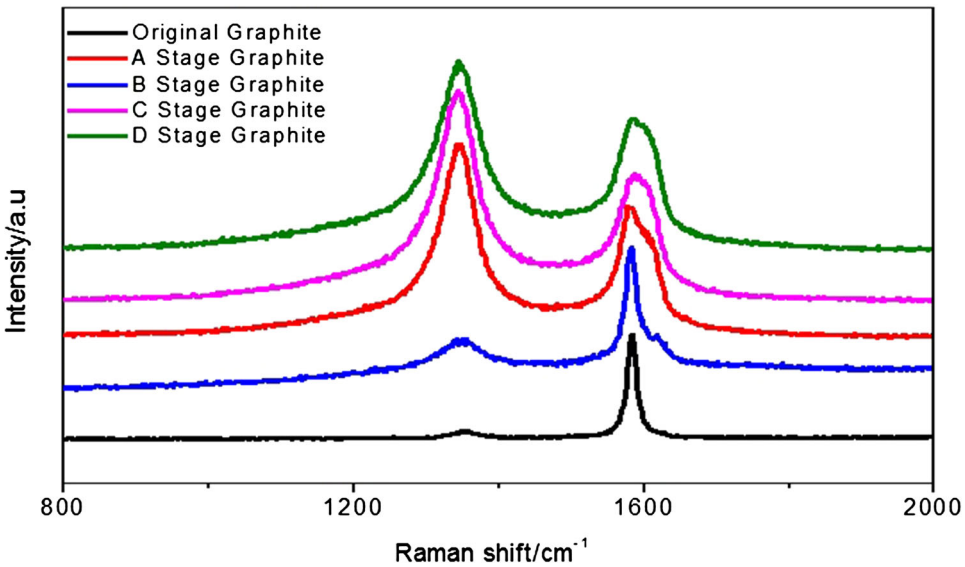

Fig. 6 Raman spectra of graphite particles before and after the test

$I_G = 1.019$) is the smallest among all the phases, indicating that the graphitization degree of phase B is the relatively best. However, a larger graphitization degree generally indicates a better lubrication performance. So the stable phase is the most feasible graphitization stage in the tribopair operation, and lubrication effect is the optimal.

4 Conclusions

This study conducts a series of experiments on the mixed powder lubrication under optimized conditions based on previous studies using a face-to-face contact tribometer. The changes in surface roughness, element content, and carbon structure of the boundary layers formed on lower specimens have been observed and analyzed to explore the boundary layer evolution of the mixed lubrication interface. Meanwhile, some typical microforms are obtained. The following conclusions are drawn:

1. On the basis of the experimental curves of dynamic friction coefficients over time throughout the entire process, as well as the observation and analysis on the boundary layers formed on lower specimens. The evolution process of the mixed powder lubrication can be divided into four typical stages: (A) running-in, (B) stable, (C) deterioration, and (D) damage.
2. The surface roughness of the running-in, stable, and deterioration stages is less than the surface roughness at start moment and damage stage, which indicates that the lubrication performance is better, when the surface is smoother. At the same time, the height difference between the peak and valley of the boundary layers is relatively smaller, which gives more details about the boundary layer.
3. Analysis of the element composition of the boundary layers indicates the lubrication performance and boundary layers states. The carbon content of the surface decreases with the friction process, but the copper content increases. Iron could be detected on the lower specimen surface at the damage stage, showing that two friction surfaces come directly in contact and lubrication conditions deteriorate. The lack of graphite powder in the tribopairs, which could be found by carbon content, is an important reason for the lubrication deterioration and increasing of the wear.
4. Raman spectral analysis of the boundary layers shows the original ordering degree of the graphite powder is smaller than those after the test. This finding illustrates that the graphitization degree of the graphite powder

worsens after the friction and wear test. The reason for this is that its complete lamellar structure and micro-crystal structure are destroyed during the experiment by the motions, such as the extrusion, inner shearing, grinding and collision et al. Therefore, a degradation of the graphite carbon structure is another significant reason for lubrication deterioration. Simultaneously, the ordering degree of stable phase is the smallest among all the phases, indicating that the graphitization degree of this phase is the best relatively and lubrication effect is the optimal.

Acknowledgments The authors wish to thank the financial support from the National Natural Science Foundation of China (51475135). This work also partly supported by the China Postdoctoral Science Foundation (2014M550339, 2015T80647) and the Tribology Science Fund of state Key Laboratory of Tribology (SKLTKF13A02).

References

1. Nikas, G.K.: A state-of-the-art review on the effects of particulate contamination and related topics in machine-element contacts. Proc. IME. J. J. Eng. Tribol. **224**, 453–479 (2010)
2. Reches, Z., Lockner, D.A.: Fault weakening and earthquake instability by powder lubrication. Nature **467**, 452–455 (2010)
3. Renouf, M., Massi, F., Fillot, N., Saulot, A.: Numerical tribology of a dry contact. Tribol. Int. **44**, 834–844 (2011)
4. Zeng, C., Renouf, M., Berthier, Y., Hamdi, R.: Numerical investigation on the electrical transmission ability of a shearing powder layer. Granul. Matter **18**, 7 (2016)
5. Godet, M.: The third-body approach: a mechanical view of wear. Wear **100**, 437–452 (1984)
6. Iordanoff, I., Berthier, Y., Descartes, S., Heshmat, H.: A review of recent approaches for modeling solid third bodies. J. Tribol. **124**, 725–735 (2002)
7. Dougherty, P.S., Marinack, M.C., Sunday, C.M., Higgs, C.F.: Shear-induced particle size segregation in composite powder transfer films. Powder Technol. **264**, 133–139 (2014)
8. Wang, W., Liu, X.J., Xie, T., Liu, K.: Effects of sliding velocity and normal load on tribological characteristics in powder lubrication. Tribol. Lett. **43**, 213–219 (2011)
9. Renouf, M., Cao, H.P., Nhu, V.H.: Multiphysical modeling of third-body rheology. Tribol. Int. **44**, 417–425 (2011)
10. Reddy, N.S.K., Rao, P.V.: Performance improvement of end milling using graphite as a solid lubricant. Mater. Manuf. Process. **20**, 673–686 (2005)
11. Iordanoff, I., Elkholy, K., Khonsari, M.M.: Effect of particle size dispersion on granular lubrication regimes. Proc. IME. J. J. Eng. Tribol. **222**, 725–739 (2008)
12. Higgs, C., Tichy, J.: Effect of particle and surface properties on granular lubrication flow. Proc. IME. J. J. Eng. Tribol. **222**, 703–713 (2008)
13. Wornyoh, E.Y.A., Jasti, V.K., Higgs, C.F.: A review of dry particulate lubrication: powder and granular materials. J Tribol. T Asme. **129**, 438–449 (2007)
14. Marinack, M.C., Higgs, C.F.: Three-dimensional physics-based cellular automata model for granular shear flow. Powder Technol. **277**, 287–302 (2015)
15. Heshmat, H.: The quasi-hydrodynamic mechanism of powder lubrication. 2: lubricant film pressure profile. Lubric. Eng. **48**, 373–383 (1992)
16. Heshmat, H., Brewe, D.E.: Performance of a powder lubricated journal bearing with ws_2 powder: experimental study. J. Tribol. **118**, 484–491 (1996)
17. Heshmat, H., Brewe, D.E.: Performance of powder-lubricated journal bearings with MoS_2 powder—experimental-study of thermal phenomena. J. Tribol. Trans. ASME. **117**, 506–512 (1995)
18. Kounoudji, K.A., Renouf, M., Mollon, G., Berthier, Y.: Role of third body on bolted joints' self-loosening. Tribol. Lett. **61**, 1–8 (2016)
19. Colas, G., et al.: How far does contamination help dry lubrication efficiency? Tribol. Int. **65**, 177–189 (2013)
20. Zhang, Y.W., Li, Z.P., Yan, J.C., Ren, T.H., Zhao, Y.D.: Tribological behaviours of surface-modified serpentine powder as lubricant additive. Ind. Lubr. Tribol. **68**, 1–8 (2016)
21. Podgornik, B., Kosec, T., Kocijan, A., Donik, C.: Tribological behaviour and lubrication performance of hexagonal boron nitride (h-bn) as a replacement for graphite in aluminium forming. Tribol. Int. **81**, 267–275 (2015)
22. Paulus, A.C., et al.: Pmma third-body wear after unicondylar knee arthroplasty decuples the uhmwpe wear particle generation in vitro. Biomed. Res. Int. **2015**, 1–7 (2015)
23. Meng, F.J., Liu, K., Wang, W.: The force chains and dynamic states of granular flow lubrication. Tribol. Trans. **58**, 70–78 (2015)
24. Descartes, S., Godeau, C., Berthier, Y.: Friction and lifetime of a contact lubricated by a solid third body formed from an $MoS_{1.6}$ coating at low temperature. Wear **330**, 478–489 (2015)
25. Descartes, S., Berthier, Y.: Rheology and flows of solid third bodies: background and application to an $MoS_{1.6}$ coating. Wear **252**, 546–556 (2002)
26. Higgs, C.F., Heshmat, H.: Characterization of pelletized MoS_2 powder particle detachment process. J. Tribol. **123**, 455–461 (2001)
27. Patrick, S.M., Dougherty, P.S.M., Pudjoprawoto, R., Higgs, C.F.: An investigation of the wear mechanism leading to self-replenishing transfer films. Wear **272**, 122–132 (2011)
28. Pudjoprawoto, R., Dougherty, P., Higgs, C.F.: A volumetric fractional coverage model to predict frictional behavior for in situ transfer film lubrication. Wear **304**, 173–182 (2013)
29. Wang, W., Liu, X., Liu, K.: Surface observations of a powder layer during the damage process under particulate lubrication. Wear **297**, 841–848 (2013)
30. Reddy, N.S.K., Rao, P.V.: Experimental investigation to study the effect of solid lubricants on cutting forces and surface quality in end milling. Int. J. Mach. Tools Manuf **46**, 189–198 (2006)
31. Gopal, A.V., Rao, P.V.: Performance improvement of grinding of sic using graphite as a solid lubricant. Mater. Manuf. Process. **19**, 177–186 (2004)
32. Kimura, R., Yoshida, M., Sasaki, G., Pan, J., Fukunaga, H.: Characterization of heat insulating and lubricating ability of powder lubricants for clean and high quality die casting. J. Mater. Process. Technol. **130**, 289–293 (2002)
33. Pinheiro, C.A.M., Samarasekera, I.V., Brimacombe, J.K., Walker, B.N.: Mould heat transfer and continuously cast billet quality with mould flux lubrication—part 1—mould heat transfer. Ironmak. Steelmak. **27**, 37–54 (2000)